UC Santa Barbara
UC Santa Barbara Previously Published Works

Title

Controlled drug release to cancer cells from modular one-photon visible light-responsive micellar system

Permalink

https://escholarship.org/uc/item/9dg357xg

Journal

Chemical Communications, 52(69)

ISSN

1359-7345

Authors

Poelma, Saemi O
Oh, Seung Soo
Helmy, Sameh
et al.

Publication Date

2016-08-18

DOI

10.1039/c6cc04127b

Peer reviewed

Controlled drug release to cancer cells from modular one-photon visible light-responsive micellar system†

Saemi O. Poelma,‡[a] Seung Soo Oh,‡[b] Sameh Helmy,[a] Abigail S. Knight,[b]
G. Leslie Burnett,[b] H. Tom Soh,*[bc] Craig J. Hawker*[ab] and Javier Read de Alaniz*[a]

We present a one-photon visible light-responsive micellar system for efficient, on-demand delivery of small molecules. Release is mediated by a novel class of photochromic material – donor–acceptor Stenhouse adducts (DASAs). We demonstrate controlled delivery of small molecules such as the chemotherapeutic agent (paclitaxel) to human breast cancer cells triggered by micellar switching with low intensity, visible light.

Polymeric nanocarrier systems such as micelles and vesicles offer many advantages for delivery of therapeutic agents as they increase bioavailability, extend circulation times and minimize side effects.[1] In particular, light-activated drug release systems have garnered recent interest[2] driven by the non-invasive nature of light and the ability to offer temporal and spatial control. For successful light-mediated systems, drug release can be achieved at particular locations and at specific times leading to a reduction of side effects for potent toxic drugs (*e.g.*, chemotherapeutic agents such as paclitaxel).[3]

Previously, light-mediated drug delivery systems have been based on photoresponsive groups, such as *o*-nitrobenzyl and coumarin-based groups,[4] azobenzene[5] or spiropyran.[6] A non-reversible hydrophobic to hydrophilic switch has also been reported involving the Wolff rearrangement of 2-diazo-1,2-naphthoquinone (DNQ) units.[7] However, an inherent drawback of these traditional systems arises from their reliance on ultraviolet (UV) light, which not only has the potential to harm healthy cells but also suffers from poor tissue penetration.[8] Alternative strategies that enable the use of wavelengths that penetrate deeper through tissue while simultaneously offering low phototoxicity would therefore be a major advance.[9]

To date, a number of controlled drug release systems have been reported using longer wavelength light. They include systems using upconverted UV light,[10] noble metal-based nanocarriers[11] or two-photon excitation.[12] Although these systems have demonstrated photocontrol with NIR, the process is less efficient than the direct excitation systems based on UV light.[12a] As a consequence, extended irradiation with high laser powers are required to trigger the disassembly of the photoresponsive nanocarriers, resulting in harmful heating effects that lead to unwanted cell death.[10] Furthermore, challenges associated with biocompatibility, surface functionalization and unintentional particle accumulation remains a concern for metal-based nanocarriers.[13] Photochromic material that can be controlled with low intensity, one-photon absorption of visible or NIR light may overcome many of these challenges and improve photo-controlled targeted drug delivery systems. A challenge in implementing this strategy, however, is the lack of synthetically versatile, photo-responsive materials capable of activation with one-photon long-wavelength light.[14,15]

To address this need for new classes of photochromic materials, we recently developed the donor–acceptor Stenhouse adducts (DASA), that undergo a hydrophobic-to-hydrophilic polarity change triggered by visible light between 530 and 570 nm.[16] In addition to the more desirable wavelengths, one-photon absorption tend to be more efficient than two-photon processes with the photoisomerization of DASA systems being triggered by low intensities of light ($\sim 1\ mW\ cm^{-2}$) which opens an attractive avenue for biomedical applications.[17] In this work, DASA building blocks are used as photochromic units in the construction of polymer micelles for the controlled release of small molecules to cells by the triggered structural disassembly of micelles using one-photon visible light.

Donor–acceptor Stenhouse adducts are readily prepared by a two-step process: an "on-water" Knoevenagel condensation of a Meldrum's acid or a barbituric acid derivative with furfural to produce an activated furan, which is then treated with a secondary amine to provide highly colored DASA derivatives in excellent yield (70–90%).[18] Importantly, both the barbituric acid and the secondary amine can bear tailored functionalities

[a] *Department of Chemistry and Biochemistry, University of California, Santa Barbara, California, 93106, USA. E-mail: javier@chem.ucsb.edu*

[b] *Materials Department, Materials Research Laboratory, University of California, Santa Barbara, California, 93106, USA*

[c] *Department of Mechanical Engineering, University of California, Santa Barbara, California, 93106, USA*

that can be used to construct photochromic materials, as well as tune properties of the material. Preliminary work has shown that conjugation of a *N,N*-di-*n*-octyl-substituted DASA derivative with poly(ethylene glycol) (PEG, M_n = 3 kDa, PDI = 1.1) through copper-mediated azide alkyne cycloaddition (CuAAC) reaction leads to a visible light-responsive amphiphilic system.[16] Although this material served as an excellent proof-of-principle, we sought to increase the stability of the light-responsive amphiphilic system for our studies with living cells that require a buffered solution.

It is well-known that increasing hydrophobicity of an amphiphile leads to lower critical micelle concentration (CMC) and enhanced stability.[19] Thus, we leveraged the facile DASA synthesis to increase the hydrophobicity through a one-pot synthesis from commercially available starting materials to obtain a barbituric acid derivative **2** with two *n*-didodecyl groups. Reaction with furfural and a functionalized secondary amine leads to **3** with an azide functionality, which was subsequently conjugated to an alkyne-terminated PEG to prepare the desired amphiphilic DASA-PEG conjugate (DASA-amphiphile) **4** (Scheme 1a). We note that the CMC of DASA-amphiphile **4** prepared with *n*-didodecyl groups was approximately 5 times lower (9 μM) than that of DASA-amphiphile with *n*-dioctyl groups (49 μM).[16] Triggered by visible light, the colored hydrophobic triene form of the DASA moiety photoisomerizes into its colorless hydrophilic zwitterionic form. This significant change in polarity and solubility of the DASA moiety leads to **5**, which is doubly hydrophilic (Scheme 1b, right). Of note, this reaction is not reversible because the aqueous medium plays a significant role in solvating the closed zwitterionic isomer.[18]

Based on this functional DASA-amphiphile, we prepared a visible light-responsive micellar system that can release hydrophobic cargo (Scheme 1c).[16] In an aqueous medium, self-assembly of DASA-amphiphile into micelles occurs where hydrophilic PEG (blue) comprises the corona and hydrophobic DASAs (red) constitute the core. Visible light irradiation of aqueous samples of DASA-amphiphile induces isomerization of the DASA to its hydrophilic form, which leads to disassembly of the micelles. This process can be readily observed by the naked eye; red solution of DASA-amphiphile indicates the hydrophobic form of DASA whereas a tan solution indicates photoisomerization to the zwitterionic form. We used UV-Vis, fluorescent spectroscopy and dynamic light scattering to verify that the micellar disassembly is triggered by the photoisomerization of the DASA moieties from **4** to **5** (see ESI†). Of note, no special precautions are required for handling because ambient light does not trigger micelle disassembly without extended exposure (>3 hours).

Hydrophobic dye Nile Red was first used to demonstrate that the cargo stays encapsulated within the micelle until visible light is irradiated to trigger micelle disassembly (Fig. 1). Initially, we incubated 0.5 mg mL^{-1} of DASA-amphiphile **4** containing 6 μg mL^{-1} Nile Red with MCF-7 human breast cancer epithelial cells for 1 hour in the presence and absence of visible light. Nile Red readily penetrates cell membranes and subsequently stains intracellular lipids, emitting strong fluorescence at 530 nm.[20] To monitor the delivery of Nile Red into the cells, we performed live-cell imaging *via* fluorescence microscopy immediately after cell washing (see ESI†). In the absence of irradiation, the Nile Red remained in the micelles, and we observed minimal delivery, as evidenced by the negligible levels of fluorescence in the cells (Fig. 1a, left). In contrast, irradiation by visible light induced the disruption of micelles and allowed efficient cargo delivery into the cells, as evidenced by the strong fluorescence of Nile Red observed in the cells (Fig. 1a, right).
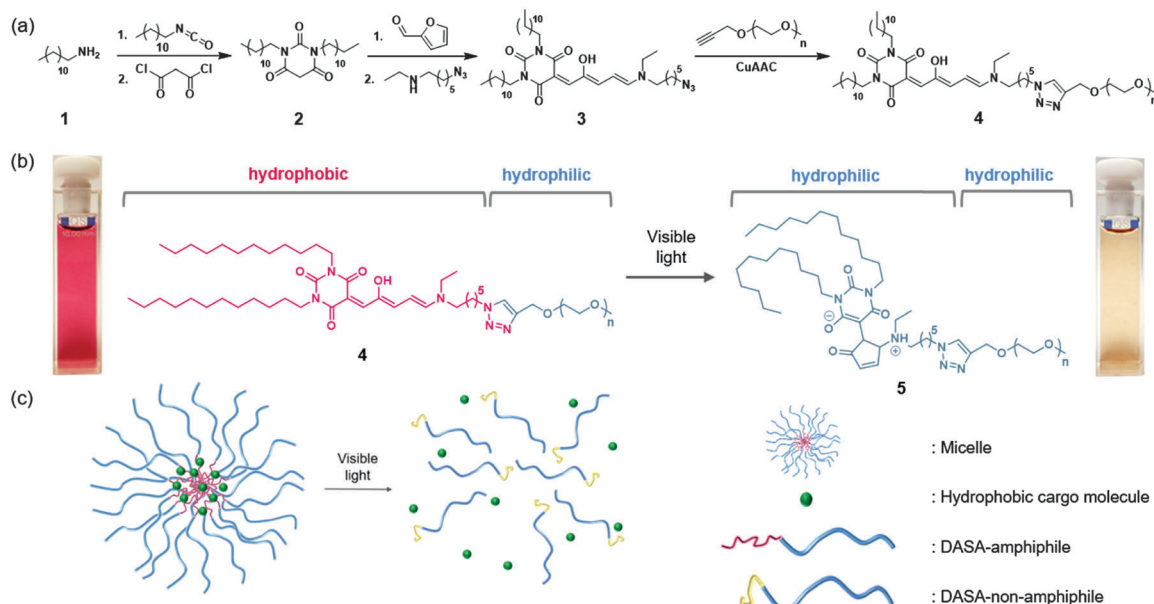
Scheme 1 (a) Synthetic route to prepare DASA-PEG conjugate **4** (DASA-amphiphile). (b) Hydrophobic DASA segment of **4** (DASA-amphiphile) photoisomerizes and becomes **5** (DASA-non-amphiphile) once irradiated with visible light, portrayed by the highly colored micelle solution (left) and tan solution (right). (c) DASA-amphiphile self-assembles into micelles in an aqueous medium to encapsulate hydrophobic cargo molecules (left). Visible light triggers the disruption of micelles and release of cargo molecules (right).
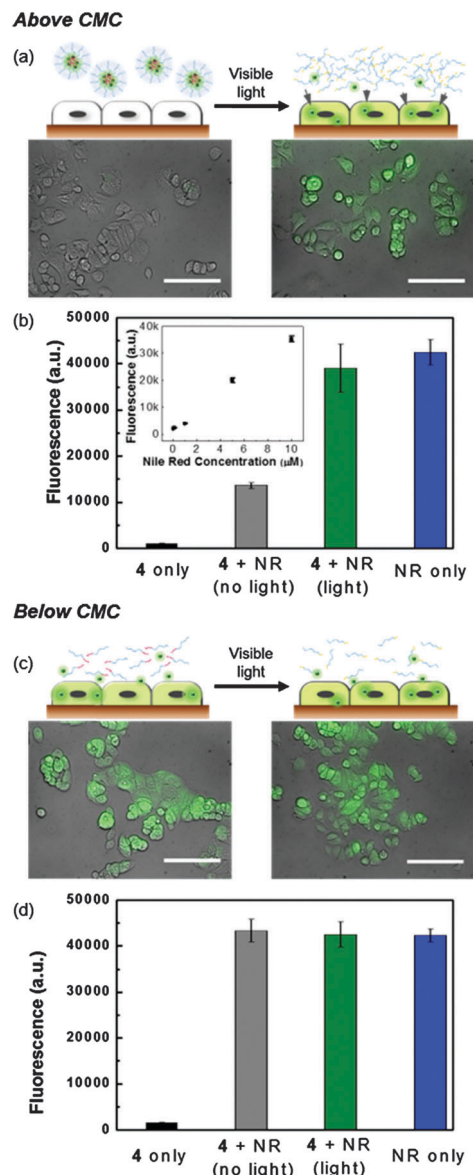
Fig. 1 Visible light-mediated cargo delivery of Nile Red (NR) into MCF-7 cells above (a and b) and below (c and d) CMC. (a) Schematic of cells incubated with DASA-amphiphile **4** above CMC before (top left) and after (top right) visible light irradiation. Corresponding fluorescence microscopy images of MCF-7 cells (bottom). Scale bar = 100 μm. (b) Linear relationship of cell fluorescence intensity to Nile Red concentration (inset). Fluorescence measurement of Nile Red in MCF-7 cells. (c) Schematic of cells incubated with DASA-amphiphile **4** below CMC before (top left) and after (top right) visible light irradiation. Corresponding fluorescence microscopy images of MCF-7 cells (bottom). Scale bar = 100 μm. (d) Fluorescence measurement of Nile Red in MCF-7 cells.

To further demonstrate the efficiency of the cargo delivery process and verify temporal control with visible light irradiation, we measured the amount of delivered cargo through the fluorescence of cell-internalized Nile Red. The fluorescence of DASA was negligible at the measured wavelength (Fig. 1b, black) and the cell fluorescence after incubation with free Nile Red and subsequent washing was proportional to the concentration of Nile Red ($0.06 \ \mu g \ mL^{-1}$ to $6 \ \mu g \ mL^{-1}$) as shown in the inset of Fig. 1b.

These results show that the observed fluorescence is primarily from Nile Red molecules that are released from the micelles and therefore fluorescence intensity is directly proportional to Nile Red concentration. We found that visible light irradiation (Fig. 1b, green) induced an approximately 300% increase in intensity compared to the absence of visible light (Fig. 1b, grey), confirming light-mediated cargo delivery to the cells.

We note that the zwitterionic DASA-amphiphile **5** does not interfere with intracellular diffusion of the unloaded cargo, which is important for achieving efficient delivery. The intensity of cells incubated with free Nile Red (Fig. 1b, blue) was comparable to that of the cells incubated with Nile Red encapsulating DASA-amphiphile **4** after visible light irradiation (Fig. 1b, green). Below the CMC ($5 \ \mu g \ mL^{-1}$) of the DASA-amphiphile **4**, we observed delivery of Nile Red into both the visible-light irradiated and the non-irradiated cells (Fig. 1c), implying no evidence of light-induced cargo delivery. Compared to the cells incubated with Nile Red only (Fig. 1d, blue), irradiation with light (Fig. 1d, green) and in the absence of light (Fig. 1d, grey) showed negligible difference in Nile Red fluorescence intensity in the cells, supporting that visible light-mediated cargo delivery requires encapsulating Nile Red into micelles.

To demonstrate controlled delivery of chemotherapeutic agents with DASA-based micelles, paclitaxel which is widely used for the treatment of many different types of tumor was used (Fig. 2).[21] We prepared $0.5 \ mg \ mL^{-1}$ solutions of DASA-amphiphile **4** containing 1 μM of paclitaxel (see Fig. S11, ESI†) and incubated MCF-7 cells with this solution for an hour with and without visible light irradiation ($\lambda = 350–800$ nm, maximum $0.9 \ mW \ cm^{-2}$, 1 hour). Following thorough washing, the cells were incubated at 37 °C for 4 days with cell viability being measured every 24 hours (live/dead assay – see ESI†).[22]

Next, we performed a series of control experiments to establish biocompatibility and viability of the DASA-amphiphile **4** for drug delivery. First we show that cells incubated with DASA-amphiphile **4** alone do not show any notable decrease of cell viability over 4 days regardless of light irradiation (Fig. 2, black and red). In addition, the viability of the cells directly exposed to DASA-amphiphile **4** for 24 hours without washing do not change significantly (Fig. S10, ESI†). The viability of the cells incubated with paclitaxel-loaded DASA-amphiphiles exposed to visible
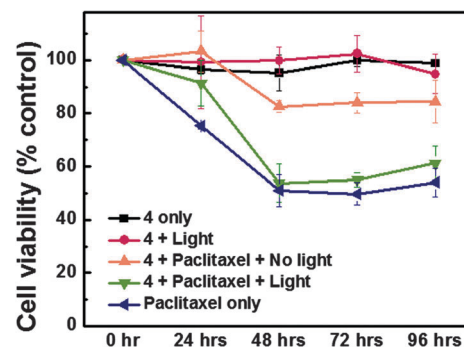

Fig. 2 Monitoring cell viability of MCF-7 breast cancer cells incubated at 37 °C for 4 d.

light (Fig. 2, green) is comparable (<3% difference) to that of the cells treated with paclitaxel alone (Fig. 2, blue), indicating the efficient drug release mediated by visible light. Importantly, cells incubated with paclitaxel-loaded DASA-amphiphiles, but not irradiated with light (Fig. 2, orange) display a significantly lower cell death over 4 days. Within 48 hours, the viability of cells irradiated with visible light decreased by 46%, approximately 3 times more than non-irradiated cells. While preparing micelles with a higher loading of paclitaxel (10 μM) led to a slightly better performance (60% decrease in cell viability), the degree of cytotoxicity when compared to the system we used (1 μM of paclitaxel led to 40% decrease in cell viability) became smaller (Fig. S12, ESI†), which presumably is due to the effective concentration of paclitaxel inhibiting the cell growth.[23]

In conclusion, we report a one-photon, visible light-responsive photochromic micellar system for efficient, on-demand drug delivery. This system uses a new class of photochromic material (DASA) which overcomes challenges associated with traditional UV light activation and multi-photon processes. The effectiveness of these light-responsive micellar materials in an *in vitro* setting was demonstrated by light controlled delivery of the chemotherapeutic agent paclitaxel to tumor cells.

Notes and references

1 (a) E. G. Kelley, J. N. Albert, M. O. Sullivan and T. H. Epps, III., *Chem. Soc. Rev.*, 2013, **42**, 7057–7071; (b) S. Mura, J. Nicolas and P. Couvreur, *Nat. Mater.*, 2013, **12**, 991–1003; (c) N. Rapoport, *Prog. Polym. Sci.*, 2007, **32**, 962–990; (d) V. P. Torchilin, *Pharm. Res.*, 2007, **24**, 1–16; (e) B. Kumar, M. A. Aga, A. Rouf, B. A. Shah and S. C. Taneja, *RSC Adv.*, 2014, **4**, 17206–17209; (f) C. J. F. Rijcken, O. Soga, W. E. Hennink and C. F. van Nostrum, *J. Controlled Release*, 2007, **120**, 131–148; (g) M. Elsabahy and K. L. Wooley, *Chem. Soc. Rev.*, 2012, **41**, 2545–2561.
2 (a) J.-F. Gohy and Y. Zhao, *Chem. Soc. Rev.*, 2013, **42**, 7117–71239; (b) W. A. Velema, W. Szymanski and B. L. Feringa, *J. Am. Chem. Soc.*, 2014, **136**, 2178–2191; (c) Y. Zhao, *Macromolecules*, 2012, **45**, 3647–3657; (d) A. Bansal and Y. Zhang, *Acc. Chem. Res.*, 2014, **47**, 3052–3060; (e) Y. Huang, R. Dong, X. Zhu and D. Yan, *Soft Matter*, 2014, **10**, 6121–6138; (f) A. Y. Rwei, W. Wang and D. S. Kohane, *Nano Today*, 2015, **10**, 451–467.
3 C. Oerlemans, W. Bult, M. Bos, G. Storm, J. F. W. Nijsen and W. E. Hennink, *Pharm. Res.*, 2010, **27**, 2569–2589.
4 For select examples, see: (a) J. Jiang, X. Tong, D. Morris and Y. Zhao, *Macromolecules*, 2006, **39**, 4633–4640; (b) J. Babin, M. Pelletier, M. Lepage, J.-F. Allard, D. Morris and Y. Zhao, *Angew. Chem., Int. Ed.*, 2009, **48**, 3329–3332; (c) D. Han, X. Tong and Y. Zhao, *Langmuir*, 2012, **28**, 2327–2331.
5 For select reviews, see: (a) D. Wang and X. Wang, *Prog. Polym. Sci.*, 2013, **38**, 271–301; (b) A. Goulet-Hanssens and C. J. Barrett, *J. Polym. Sci., Part A: Polym. Chem.*, 2013, **51**, 3058–3070.
6 For select examples, see: (a) M.-Q. Zhu, L. Zhu, J. J. Han, W. Wu, J. K. Hurst and A. D. Q. Li, *J. Am. Chem. Soc.*, 2006, **128**, 4303–4309; (b) M. Surin, P. Samori, A. Jouaiti, N. Kyritsakas and M. W. Hosseini, *Angew. Chem., Int. Ed.*, 2007, **46**, 245–249; (c) R. Tong, H. D. Hemmati, R. Langer and D. S. Kohane, *J. Am. Chem. Soc.*, 2012, **134**, 8848–8855; (d) R. Tong, H. H. Chiang and D. S. Kohane, *Proc. Natl. Acad. Sci. U. S. A.*, 2013, **110**, 19048–19053.
7 (a) A. P. Goodwin, J. L. Mynar, Y. Ma, G. R. Fleming and J. M. J. Fréchet, *J. Am. Chem. Soc.*, 2005, **127**, 9952–9953; (b) G.-Y. Liu, C.-J. Chen, D.-D. Li, S.-S. Wang and J. Ji, *J. Mater. Chem.*, 2012, **22**, 16865–16871.
8 (a) J. Kolega, *Biochem. Biophys. Res. Commun.*, 2004, **320**, 1020–1025; (b) S. O. Lock and J. V. Friend, *Food Chem. Toxicol.*, 1986, **24**, 789–793.
9 (a) R. Weissleder, *Nat. Biotechnol.*, 2001, **19**, 316–317; (b) V. G. Peters, D. R. Wyman, M. S. Patterson and G. L. Frank, *Phys. Med. Biol.*, 1990, **35**, 1317–1334.
10 (a) M. L. Viger, M. Grossman, N. Fomina and A. Almutairi, *Adv. Mater.*, 2013, **25**, 3733–3738; (b) B. Yan, J.-C. Boyer, N. R. Branda and Y. Zhao, *J. Am. Chem. Soc.*, 2011, **133**, 19714–19717.
11 For select examples, see: (a) N. Gandra, C. Portz and S. Singamaneni, *Adv. Mater.*, 2014, **26**, 424–429; (b) W.-P. Li, P.-Y. Liao, C.-H. Su and C.-S. Yeh, *J. Am. Chem. Soc.*, 2014, **136**, 10062–10075; (c) V. Vollani, G. Signore, O. Vittorio, P. Faraci, S. Luin, J. Peréz-Prieto and F. Beltram, *J. Mater. Chem. B*, 2013, **1**, 4225–4230; (d) J. Chen, Z. Guo, H.-B. Wang, M. Gong, X.-K. Kong, P. Xia and Q.-W. Chen, *Biomaterials*, 2013, **34**, 571–581; (e) R. Huschka, A. Barhoumi, Q. Liu, J. A. Roth, L. Ji and N. J. Halas, *ACS Nano*, 2012, **6**, 7681–7691; (f) J. Croissant and J. I. Zink, *J. Am. Chem. Soc.*, 2012, **134**, 7628–7631.
12 For a review on one-photon and two-photon probes, see: (a) G. Bort, T. Gallavardin, D. Ogden and P. I. Dalko, *Angew. Chem., Int. Ed.*, 2013, **52**, 4526–4537; for select examples of two-photon excitation for drug delivery, see: (b) Q. Lin, Q. Huang, C. Li, C. Bao, Z. Liu, F. Li and L. Zhu, *J. Am. Chem. Soc.*, 2010, **132**, 10645–10647; (c) S. R. Wecksler, A. Mikhailovsky, D. Korystov and P. C. Ford, *J. Am. Chem. Soc.*, 2006, **128**, 3831–3837.
13 (a) N. M. Idris, M. K. G. Jayakumar, A. Bansal and Y. Zhang, *Chem. Soc. Rev.*, 2015, **44**, 1449–1478; (b) Y. B. Zheng, B. Kiraly, P. S. Weiss and T. J. Huang, *Nanomedicine*, 2012, **7**, 751–770.
14 For review on photocontrolled release using one-photon absorption of visible or NIR light, see: J. Olejniczak, C.-J. Carling and A. Almutairi, *J. Controlled Release*, 2015, **219**, 18–30.
15 For examples using photoswitches controlled by one-photon absorption, see: (a) J. Lu, E. Choi, F. Tamanoi and J. I. Zink, *Small*, 2008, **4**, 421–426; (b) E. Aznar, R. Casasús, B. García-Acosta, M. D. Marcos, R. Martínez-Máñez, F. Sancenón, J. Soto and P. Amorós, *Adv. Mater.*, 2007, **19**, 2228–2231.
16 S. Helmy, F. A. Leibfarth, S. Oh, J. E. Poelma, C. J. Hawker and J. Read de Alaniz, *J. Am. Chem. Soc.*, 2014, **136**, 8169–8172.
17 C.-J. Carling, M. L. Viger, V. A. N. Huu, A. V. Garcia and A. Almutairi, *Chem. Sci.*, 2015, **6**, 335–341.
18 S. Helmy, S. Oh, F. A. Leibfarth, C. J. Hawker and J. Read de Alaniz, *J. Org. Chem.*, 2014, **79**, 11316–11329.
19 (a) S. M. Garg, M. R. Vakili and A. Lavasanifar, *Colloids Surf., B*, 2015, **132**, 161–170; (b) Y. J. Nikas and D. Blankschtein, *Langmuir*, 1994, **10**, 3512–3528.
20 P. Greenspan, E. P. Mayer and S. D. Fowler, *J. Cell Biol.*, 1985, **100**, 965–973.
21 J. Crown, M. O'Leary and W.-S. Ooi, *Oncologist*, 2004, **9**, 24–32.
22 S. S. Oh, B. F. Lee, F. A. Leibfarth, M. Eisenstein, M. J. Robb, N. A. Lynd, C. J. Hawker and H. T. Soh, *J. Am. Chem. Soc.*, 2014, **136**, 15010–15015.
23 S. Tommasi, A. Mangia, R. Lacalamita, A. Bellizzi, V. Fedele, A. Chiriatti, C. Thomssen, N. Kendzierski, A. Latorre, V. Lorusso, F. Schittulli, F. Zito, M. Kavallaris and A. Paradiso, *Int. J. Cancer*, 2007, **120**, 2078–2085.